Measurement of the neutron-induced fission cross-section of ^{241}Am at the time-of-flight facility n_TOF

F. Belloni[1], M. Calviani[2,3], N. Colonna[4], P. Mastinu[2], P.M. Milazzo[1,a], U. Abbondanno[1], G. Aerts[5], H. Álvarez[6], F. Alvarez-Velarde[7], S. Andriamonje[5], J. Andrzejewski[8], L. Audouin[9], G. Badurek[10], M. Barbagallo[4], P. Baumann[11], F. Bečvář[12], E. Berthoumieux[5], F. Calviño[13], D. Cano-Ott[6], R. Capote[14,15], C. Carrapiço[16], P. Cennini[3], V. Chepel[17], E. Chiaveri[3], G. Cortes[13], A. Couture[18], J. Cox[18], M. Dahlfors[3], S. David[11], I. Dillmann[9], C. Domingo-Pardo[19], W. Dridi[5], I. Duran[6], C. Eleftheriadis[20], M. Embid-Segura[6], A. Ferrari[3], R. Ferreira-Marques[17], K. Fujii[1], W. Furman[21], I. Goncalves[16], E. Gonzalez-Romero[6], A. Goverdovski[22], F. Gramegna[2], C. Guerrero[7], F. Gunsing[5], B. Haas[23], R. Haight[24], M. Heil[9], A. Herrera-Martinez[3], M. Igashira[25], E. Jericha[10], F. Käppeler[9], Y. Kadi[3], D. Karadimos[26], D. Karamanis[26], M. Kerveno[11], P. Koehler[27], E. Kossionides[28], M. Krtička[12], C. Lamboudis[20], H. Leeb[10], A. Lindote[17], I. Lopes[17], M. Lozano[29], S. Lukic[11], J. Marganiec[8], S. Marrone[4], T. Martínez[7], C. Massimi[30], M.H. Meaze[4], A. Mengoni[3,14], C. Moreau[1], M. Mosconi[9], F. Neves[17], H. Oberhummer[10], S. O'Brien[18], C. Papachristodoulou[26], C. Papadopoulos[31], C. Paradela[6], N. Patronis[26], A. Pavlik[32], P. Pavlopoulos[33], L. Perrot[5], M.T. Pigni[27], R. Plag[9], A. Plompen[34], A. Plukis[5], A. Poch[13], J. Praena[29], C. Pretel[13], J. Quesada[29], T. Rauscher[35], R. Reifarth[24], M. Rosetti[36], C. Rubbia[37], G. Rudolf[11], P. Rullhusen[34], J. Salgado[16], C. Santos[16], L. Sarchiapone[3], I. Savvidis[20], C. Stephan[38], G. Tagliente[4], J.L. Tain[19], D. Tarrio(6), L. Tassan-Got[38], L. Tavora[16], R. Terlizzi[4], G. Vannini[30], P. Vaz[16], A. Ventura[36], D. Villamarin[7], M.C. Vincente[7], V. Vlachoudis[3], R. Vlastou[31], F. Voss[9], S. Walter[9], M. Wiescher[18], and K. Wisshak[9]

1   Istituto Nazionale di Fisica Nucleare (INFN), Trieste, Italy
2   Istituto Nazionale di Fisica Nucleare (INFN), Laboratori Nazionali di Legnaro, Italy
3   CERN, Geneva, Switzerland
4   Istituto Nazionale di Fisica Nucleare (INFN), Bari, Italy
5   CEA, Irfu, Gif-sur-Yvette, France
6   Universidade de Santiago de Compostela, Spain
7   Centro de Investigaciones Energeticas Medioambientales y Technologicas, Madrid, Spain
8   University of Lodz, Lodz, Poland
9   Karlsruhe Institute of Technology, Campus Nord, Institut für Kernphysik, Germany
10 Atominstitut der Österreichischen Universitäten, Technische Universität Wien, Austria
11 Centre National de la Recherche Scientifique/IN2P3 - IReS, Strasbourg, France
12 Faculty of Mathematics and Physics, Charles University in Prague, Czech Republic
13 Universitat Politecnica de Catalunya, Barcelona, Spain
14 International Atomic Energy Agency (IAEA), NAPC/Nuclear Data Section, Vienna, Austria
15 Universidad de Sevilla, Spain
16 Instituto Tecnológico e Nuclear (ITN), Lisbon, Portugal
17 LIP - Coimbra & Departamento de Fisica da Universidade de Coimbra, Portugal
18 University of Notre Dame, Notre Dame, USA
19 Instituto de Física Corpuscular, CSIC-Universidad de Valencia, Spain
20 Aristotle University of Thessaloniki, Greece
21 Joint Institute for Nuclear Research, Frank Laboratory of Neutron Physics, Dubna, Russia
22 Institute of Physics and Power Engineering, Obninsk, Russia
23 Centre National de la Recherche Scientifique/IN2P3 - CENBG, Bordeaux, France
24 Los Alamos National Laboratory, New Mexico, USA
25 Tokyo Institute of Technology, Tokyo, Japan
26 University of Ioannina, Greece
27 Oak Ridge National Laboratory, Oak Ridge, USA
28 NCSR, Athens, Greece
29 Universidad de Sevilla, Spain
30 Dipartimento di Fisica, Università di Bologna and Sezione INFN di Bologna, Italy
31 National Technical University of Athens, Greece
32 Institut für Fakultät für Physik, Universität Wien, Austria
33 Pôle Universitaire Léonard de Vinci, Paris La Défense, France

[34] CEC-JRC-IRMM, Geel, Belgium
[35] Department of Physics and Astronomy, University of Basel, Switzerland
[36] ENEA, Bologna, Italy
[37] Università degli Studi di Pavia, Pavia, Italy
[38] Centre National de la Recherche Scientifique/IN2P3 - IPN, Orsay, France

Abstract. The neutron-induced fission cross-section of ^{241}Am has been measured relative to the standard fission cross-section of ^{235}U between 0.5 and 20 MeV. The experiment was performed at the CERN n_TOF facility. Fission fragments were detected by a fast ionization chamber by discriminating against the α-particles from the high radioactivity of the samples. The high instantaneous neutron flux and the low background of the n_TOF facility enabled us to obtain uncertainties of $\approx 5\%$. With the present results it was possible to resolve discrepancies between previous data sets and to confirm current evaluations, thus providing important information for design studies of future reactors with improved fuel burn-up.

1 Introduction

The growth in world energy consumption implies pressing problems that humanity has to face in the next decades. On the one hand, it is mandatory to balance the energy demand between developed Countries and the majority of the world population, on the other side the environmental impact of the extensive use of fossil fuels must be strongly reduced. Recent analyses have also shown that the tipping point of oil production is very close or could have already passed [1]. In this scenario nuclear energy may play an important role in the future as a part of the global energy mix. Moreover, the energy from nuclear reactors, in conjunction with renewable energy sources, may make it possible to achieve a reduction of CO_2 emission responsible for the greenhouse effect.

However, nuclear safety and non-proliferation are still of concern for the public acceptance of this energy source. In particular, the long-term hazard of nuclear waste needs a clear solution. High-level radioactive waste remains for thousands of years and must be kept reliably isolated from the biosphere. Although the geological disposal could be a possible solution, alternative chances arise from the realization of Advanced Generation-IV reactors based on fast neutron spectra [2]. In this case the production of Minor Actinides (MA) can be significantly reduced via neutron-induced fission. Other solutions depend on the use of dedicated systems for spent fuel reprocessing, partitioning, and incineration of MAs. The development of such reactors requires an accurate and consistent knowledge of neutron-induced fission cross-sections of heavy nuclei over a wide energy range.

The neutron-induced fission cross-section of the MA isotope ^{241}Am plays an important role in the study of reactors such as the ADvanced Minor Actinide Burner (ADMAB) or the Sodium-cooled Fast Reactor (SFR). Sensitivity studies for innovative systems [3–5] showed that the fission cross-section of ^{241}Am is required with accuracies of 1.5–5% in the energy range between 1 and

20 MeV for the design of ADMAB reactors, while there are less restrictive requests of 6–7% accuracy for the SFR case.

The fission cross-section of ^{241}Am has been repeatedly investigated [6–15], but so far these data exhibit severe discrepancies with respect to the absolute value of the cross-section as well as to the exact energy position of the fission threshold. Systematic uncertainties are mostly dominated by the high α activity of ^{241}Am and by isotopic impurities in the samples. Accordingly, the evaluated cross-sections in the data libraries suffer from the limited experimental accuracy as well.

In view of this unsatisfactory situation, an extensive measurement campaign for reducing the uncertainties of the fission cross-section of ^{241}Am has been carried out at the neutron time-of-flight facility n_TOF at CERN, which is unique for its very high instantaneous neutron flux and extremely low duty cycle. These features are instrumental for reducing the α background from the activity of the sample. Moreover, the good energy resolution at n_TOF is essential for a reliable determination of the fission threshold of ^{241}Am near 0.5 MeV.

Experimental set-up and data analysis procedures are described in sects. 2 and 3, respectively. The results are compared in sect. 4 to previous cross-section data in the energy range from 500 keV to 20 MeV.

2 The experimental set-up

The spallation neutron time-of-flight n_TOF facility [16] is using the pulsed beam from the CERN Proton Synchrotron (PS) accelerator, which is directed onto a massive lead target surrounded by a water layer as coolant and moderator of the neutron spectrum. The features of the n_TOF neutron beam are determined by the characteristics of the PS accelerator, *i.e.* the high energy of 20 GeV, the low duty cycle (1 pulse every 2.4 s), and an extremely high peak current of 7×10^{12} protons per bunch within a

---

[a] e-mail: `paolo.milazzo@ts,infn.it`

Table 1. Characteristics of the samples used in the ^{241}Am(n, f) measurement; the ^{235}U sample has been used as reference.

Sample	Chemical form	Mass (mg)	Thickness (μg/cm^2)	Uncertainty (%)
^{241}Am	AmO$_2$	0.234	4.65	1.2
^{241}Am	AmO$_2$	0.230	4.57	1.2
^{241}Am	AmO$_2$	0.280	5.57	1.2
^{241}Am	AmO$_2$	0.279	5.56	1.2
^{241}Am	AmO$_2$	0.304	6.04	1.2
^{241}Am	AmO$_2$	0.336	6.69	1.2
^{241}Am	AmO$_2$	0.321	6.38	1.2
^{241}Am	AmO$_2$	0.277	5.52	1.2
^{235}U	U$_3$O$_8$	15.2	303	1.4
^{235}U	U$_3$O$_8$	16.6	330	1.3

short pulse width of 6 ns rms. With these parameters, an instantaneous flux of 10^5 neutrons/cm^2/pulse is reached at the sample position 187 m downstream of the spallation target. Especially the extremely low duty factor of the n_TOF facility is crucial for reducing the high α background from the activity of the ^{241}Am sample.

The evacuated neutron beam line between the spallation target and the experimental area is equipped with two collimators at 135 and 175 m, a 1.5 T sweeping magnet for removing relativistic charged particles, and thick iron and concrete shielding walls [17] for background reduction. The beam line is extended 12 m beyond the experimental area to minimize the effect of back-scattered neutrons.

The measurement has been performed with a stack of fast ionization chambers in a common housing; this set-up allowed the simultaneous measurement on several isotopes [21]. Each chamber consists of a central Al cathode 100 μm in thickness plated on both sides with sample material, and two 15 μm thick Al anodes at a distance of 5 mm from the cathode for the definition of the electric field. The electrodes are 12 cm in diameter, while the 8 cm diameter of the sample deposit matches the size of the neutron beam. The detector set-up is operated with a gas mixture of 90% Ar and 10% CF$_4$ at a pressure of 720 mbar.

The samples were prepared at the Institute of Physics and Power Engineering in Obninsk (Russia) by means of the painting technique. This coating technique was chosen to keep losses of material in the production process at a minimum. Moreover, repeated painting of the substrate using low concentration painting solutions ensures a good uniformity (5–10%) of the sample thickness. The eight ^{241}AmO$_2$ samples with a total mass of 2.261 mg consisted of material with a ^{241}Am/Am enrichment higher than 96%, whereas the two ^{235}U reference samples were isotopically pure (99.992%). The specific α activity of the ^{241}AmO$_2$ samples was 112 MBq/mg. More informations on the samples used in the present measurement are given in table 1.

The data acquisition system was based on fast digitizers operating at 10^8 samples/s [18]. The data from the digitizers were reduced by a zero-suppression routine and the remaining signals were stored for off-line analysis of the deposited energy in the detectors and the respective time of flight (TOF).

3 Data analysis

Fission events were identified by detection of fission fragments, which deposited part of their energy in the gas of the detector and the corresponding neutron energy was obtained from the respective TOF along flight path between the spallation target and the experimental area. In this way, each fission event was characterized by the energy deposited in the detector and the associated TOF.

The neutron energy was determined by means of the TOF-energy relation provided by the calibration of ref. [19], which is based on the neutron production mechanism in the spallation target and the subsequent moderation process [17], where the effective flight path is obtained via the well-known ^{235}U resonances.

Major difficulties in data analysis were related to energy losses in the samples and to pile-up signals produced by the high background of α-particles from the decay of ^{241}Am, which were investigated by realistic FLUKA [20] Monte Carlo simulations of the detector response [21]. In these simulations, kinetic energies and fragment masses were randomly generated according to the respective distributions [22] to evaluate the corrections for absorption losses in the samples and for the threshold effect imposed by the α activity (see fig. 1 of ref. [23]). With a threshold of 50 MeV in the deposited energy spectrum the α component could be completely separated from the measured fission yields, but at the expense of a reduction in detection efficiency of 50%. Moreover, the effect of α pile-up was removed by means of off-line analysis routines of the charge and amplitude signals, by which spurious events could be separated from α or fission fragment signals [24].

The ^{241}Am(n, f) cross-section has been extracted relative to the ^{235}U(n, f) cross-section, which is an established standard in the neutron energy range from 150 keV to 200 MeV [25]. Compared to a direct measurement, the ratio method has the advantage that systematic uncertainties are strongly reduced, especially with respect to the determination of the neutron flux. In this work, all samples were exposed to the same neutron flux and were measured with nearly identical detectors showing very similar signal shapes.

The ^{241}Am(n, f) cross-section has been obtained as

$$\sigma_{241}(n, f) = c(E_n) \cdot \sigma_{235}(n, f) \cdot \frac{N_{241}}{N_{235}} \cdot \frac{m_{235}}{m_{241}} \cdot \frac{A_{241}}{A_{235}}.$$

Here $c(E_n)$ is a correction factor that takes into account the dead-time effects, and $\sigma_{235}(n, f)$ is the tabulated ENDF/B-VII.0 version of the ^{235}U(n, f) cross-section that was used as a standard [26]. N denotes the number of detected fission events, m the sample masses, and A the mass numbers of the investigated isotopes.

The data acquisition system used at n_TOF is based on flash ADCs [18] with the advantage that dead-time problems are strongly reduced. In this work the signal reconstruction routine was operated with a resolution time of 270 ns. The dead-time correction has been evaluated by means of a non-paralyzable model, where the instantaneous count rate was determined for each sample as a function of neutron energy, resulting in average dead-time corrections of $\approx 6\%$.

The detection efficiency depends on the sample thickness and on the 50 MeV threshold adopted in the analysis for the deposited energy. From the performed Monte Carlo simulations [21] the efficiencies were found to be 50.7% and 45.3% for ^{241}Am and ^{235}U, respectively. The resulting efficiency correction is 5.4%.

The uncertainties of the present ^{241}Am(n, f) cross-section are determined by contributions related to the sample masses, the ^{235}U(n, f) reference cross-section, counting statistics, dead-time corrections, detection efficiency, and, predominantly, the high α activity of the sample.

The determination of the sample masses by α spectroscopy led to an uncertainty of 1.8% with contributions of 1.2% and 1.35% from ^{241}Am and ^{235}U, respectively. The only impurity that could affect the results in the fission threshold region is a trace of 0.15% of ^{239}Pu; in particular, this impurity can bring a contribution to the cross-section of 1.5% at the lowest energy value considered in the present analysis (500 keV) and smaller than 1% above 700 keV. The uncertainty of the ^{235}U reference cross-section is $\approx 2\%$ in the energy region of this analysis.

The uncertainty in neutron energy results from the time resolution of the initial proton beam and increases from about 0.1% at 0.5 MeV to 0.6% at 20 MeV [17]. The data are given with a variable bin resolution per energy decade so as to reduce the statistical uncertainty per bin to $\approx 2\%$. The dead-time and detection efficiency corrections contribute an uncertainty of the order of 1% each.

The largest systematic uncertainty of 4% results from the high α activity of the sample, which clearly dominates the $\approx 5\%$ uncertainty of the present ^{241}Am(n, f) cross-section data.

# 4 Results

The neutron-induced fission cross-section of ^{241}Am was determined with the ratio method in the energy range between 0.5 and 20 MeV. The measured cross-section ratios $\sigma_{^{241}\mathrm{Am}}(n, f)/\sigma_{^{235}\mathrm{U}}(n, f)$ and the corresponding values for the ^{241}Am fission cross-section are listed in table 2 together with the total uncertainties.

The present results are compared with previous data and evaluations in figs. 1, 2 and 3 and in table 3, where energy-integrated cross-sections in the region of overlap with the various data sets are reported. Because of the limited counting statistics the data have to be given on a rather coarse neutron energy grid.

Table 2. The cross-section ratio $\sigma(^{241}\mathrm{Am})/\sigma(^{235}\mathrm{U})$ and the deduced ^{241}Am(n, f) cross-section. Results are given with a resolution of 20 bins per energy decade up to 1 MeV; above this value the bin resolution has been fixed in order to keep the statistical uncertainty below 2%.

Energy bin (MeV)	^{241}Am$(n, f)/^{235}$U(n, f)	^{241}Am(n, f) (b)
0.501–0.562	0.17±0.02	0.19±0.02
0.562–0.631	0.19±0.02	0.21±0.02
0.631–0.708	0.31±0.02	0.35±0.02
0.708–0.794	0.55±0.03	0.61±0.03
0.794–0.891	0.78±0.03	0.87±0.04
0.891–1.03	1.07±0.04	1.25±0.04
1.03–1.26	1.39±0.03	1.66±0.03
1.26–1.63	1.51±0.03	1.85±0.03
1.63–2.24	1.44±0.02	1.83±0.03
2.24–3.16	1.46±0.02	1.82±0.03
3.16–4.47	1.58±0.04	1.83±0.04
4.47–6.31	1.68±0.05	1.79±0.05
6.31–9.17	1.45±0.04	2.51±0.07
9.17–15.40	1.31±0.04	2.31±0.06
15.40–31.62	1.11±0.02	2.39±0.05
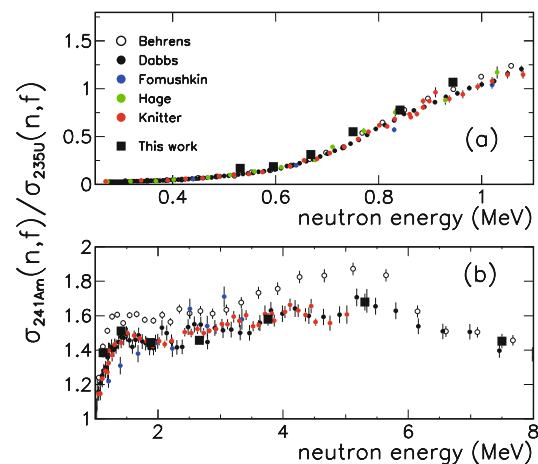
Fig. 1. (Color online) Comparison of the present cross-section ratios $\sigma(^{241}\mathrm{Am})/\sigma(^{235}\mathrm{U})$ with previous measurements [7, 11–14].

4.1 Comparison with previous measurements

The comparison with the most significant cross-section data from past measurements has been made preferentially for the ^{241}Am$(n, f)/^{235}$U(n, f) ratio to avoid systematic effects in the determination of the ^{241}Am(n, f) cross-section due the choice of the ^{235}U(n, f) reference cross-section. Good agreement has been found with previous data [7, 11–14] in the energy range around the fission threshold (upper panel of fig. 1). In the region of the first
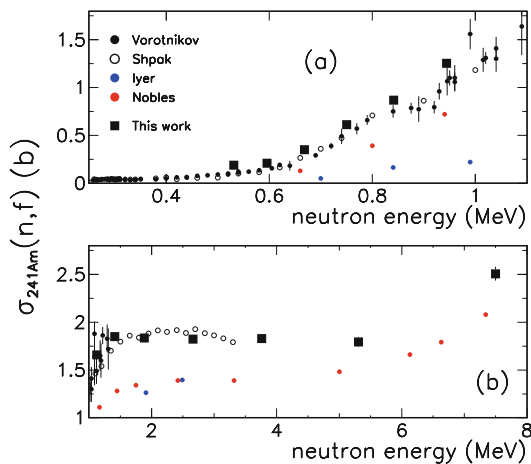
Fig. 2. (Color online) The present fission cross-section of ^{241}Am (full squares) compared with previous measurements [6, 8,10,15]. For the data reported in refs. [6,10] information on related uncertainties are not available.

fission plateau the present results are in good agreement with some of the data [11,14] while discrepancies of $\approx 10\%$ are found with respect to the cross-section ratios reported by [7,12] (lower panel of fig. 1).

The absolute fission cross-sections of ^{241}Am derived from the n_TOF results using the ^{235}U(n, f) cross-section from ENDF/B-VII.0 are presented in fig. 2 with previous data from [6,8,10,15], which had been obtained with different techniques. Fair agreement is found with [8,15], while the results of refs. [6,10] appear to deviate significantly.

Above 5 MeV only two measurements have been performed, but they are in disagreement [12,14]. In particular data from ref.[12] are approximately 10% higher than those in ref.[14]. In spite of the broad bin width the present data are supporting the results of Dabbs *et al.* [14].

For the more complete data sets available for the cross-section, the average differences to previous measurements are summarized in table 3 by comparison of the energy-integrated cross-sections over the energy range of overlap.

4.2 Evaluated data and EMPIRE calculations

The comparison of the present results with the most recent evaluation of the fission cross-section of ^{241}Am from the ENDF/B-VII.1 data library [27,28] in fig. 3 shows good agreement over the entire energy range. This evaluation is based on a theoretical analysis optimized on available experimental data up to 8 MeV; above this energy only theoretical values have been used. The agreement of the present data with those of ref. [14] confirms the reliability of this evaluation in the high neutron energy range.

Figure 3 presents also a calculation of the fission cross-section of ^{241}Am with the Arcole version of the EMPIRE code, which complements the analysis of Am isotopes inside the EMPIRE framework; previous results
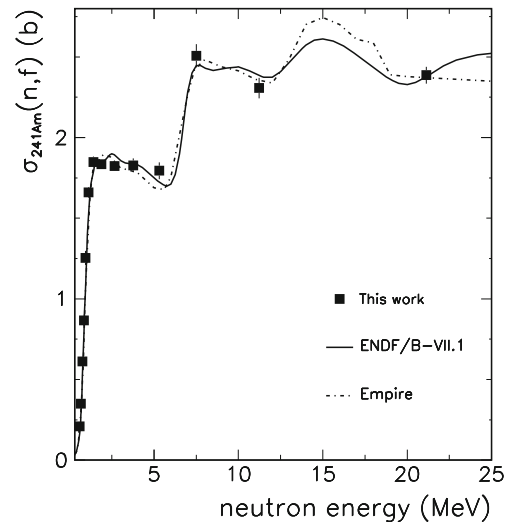
Fig. 3. Comparison of the present cross-section results (full squares) with the most recent ENDF/B-VII.1 evaluation [27] and with a calculation using the EMPIRE code [29].

Table 3. Differences between the present and previous energy-integrated cross-sections in the energy range of overlap.

Authors	Ref.	Energy range (MeV)	Difference (%)
Nobles *et al.*	[6]	0.5–7.34	+22.4
Fomushkin and Gutnikova	[7]	0.5–3.62	+0.9
Shpak *et al.*	[8]	0.5–3.3	+1.1
Knitter *et al.*	[11]	0.5–2.65	−3.9
Behrens and Browne	[12]	0.5–20.	−9.7
Dabbs *et al.*	[14]	0.5–18.7	−1.8

Table 4. Heights (V_i) and curvatures ($\hbar\omega_i$) of the two-humped fission barriers used in the simulation with the EMPIRE code [29] for the three nuclei of interest. Indices A and B refer to the inner and outer barrier and I to intermediate isomeric well. Heights and curvatures are in MeV.

Compound nucleus	V_A	$\hbar\omega_A$	V_I	$\hbar\omega_I$	V_B	$\hbar\omega_B$
^{242}Am	6.39	0.57	1.39	0.55	5.78	0.45
^{241}Am	6.17	0.77	1.33	0.54	5.82	0.57
^{240}Am	5.65	0.75	1.12	0.53	5.45	0.50

have been presented in the study of the fission cross-section of ^{243}Am [23]. The nuclear reaction model code EMPIRE [29] describes the penetrability of fission barriers with the optical model for fission, allowing for a partial damping of the resonances in the second well. For the description of the (n, f) cross-section of ^{241}Am up to 20 MeV, the contributions of the (n, f), $(n, n'f)$, and $(n, 2nf)$ channels were taken into account. Table 4 shows heights, V_i, and curvatures, $\hbar\omega_i$, of the two-humped fission barriers for the three fissioning compound nuclei ^{242}Am, ^{241}Am and ^{240}Am, respectively.

It was found that the barrier parameters of ^{241,242}Am compare well with the nominal values of the EMPIRE code [30]; the inner peak of the fission barrier of ^{240}Am is about 89% of the arithmetic mean of the literature values quoted in ref. [30], while the outer peak is in very good agreement with the corresponding mean value. The additional ingredients of the fission calculation, *i.e.* the discrete transition states at the barriers and the corresponding level densities were taken from the EMPIRE library. The present results are equally well reproduced by the ENDF/B-VII.1 evaluation and by the EMPIRE calculation.

5 Conclusions

The fission cross-section of ^{241}Am has been measured at the CERN n_TOF facility relative to that of ^{235}U in the energy range between 0.5 and 20 MeV with uncertainties of $\approx 5\%$. This experiment took advantage of the unique duty cycle of the n_TOF facility. The low repetition rate of only 0.4 Hz in combination with a digitized data acquisition system allowed for an unprecedented suppression of the α background from the sample activity. The coarse energy grid of the present results, which depends on limited counting statistics, is expected to be significantly improved in measurements at the new, future n_TOF flight path at only 20 m from the spallation target.

The results are found in good agreement with the data reported from several previous measurements as well as with the most recent evaluations. The latter point suggests that these evaluations were based on a proper selection of the data in the literature.

References

1. J. Murray, D. King, Nature **481**, 433 (2012).
2. *Accelerator-driven Systems (ADS) and Fast Reactors (FR) in Advanced Nuclear Fuel Cycles: A Comparative Study*, NEA report 3109, OECD Nuclear Energy Agency, Paris (2002) ISBN 92-64-18482-1.
3. M. Salvatores, *Uncertainty and target accuracy assessment for innovative systems using recent covariance data evaluations*, Nucl. Sc. NEA/WPEC-26 (2008) ISBN 978-92-64-99053-1, available at `www.nea.fr/html/science/wpec/volume26/volume26.pdf`.
4. G. Aliberti, G. Palmiotti, M. Salvatores, in *Proceedings of the Conference NEMEA-4, Neutron measurements, evaluations and applications, Prague (2007), JRC Scientific and Technical Reports*, edited by A. Plompen, Vol. **113** (2008) EUR23235 EN-2008.
5. S. Ganesan, H. Wienke, J. Nucl. Sci. Technol. **2**, 951 (2002).
6. R.A. Nobles, R.L. Henkel, R.K. Smith, Phys. Rev. **99**, 616 (1955).
7. E.F. Fomushkin, E.K. Gutnikova, Yad. Fiz. **10**, 917 (1969) Sov. J. Nucl. Phys. **10**, 529 (1970).
8. D.L. Shpak, Ju.B. Ostapenko, G.N. Smirenkin, Zh. Eksp. Teor. Fiz., Pis'ma Red. **9**, 196 (1969).
9. M.Cance, D.Gimat, G.Grenier, D.Parisot, in *Proceedings of the 3rd All-Union Conference on Neutron Physics, Kiev 9-13 June 1975*, Vol. **5** (1976) p. 363.
10. R.H. Iyer, R. Sampathkumar, N.K. Chaudhuri, Prog. B.A.R.C., Trombay report series No. 872 (1976) p. 106.
11. H.H. Knitter, C. Budtz-Jorgensen, Atomkernenergie **33**, 205 (1979) Nucl. Instrum. Methods Phys. Res.7811979.
12. J.W. Behrens, J.C. Browne, Nucl. Sci. Eng. **77**, 444 (1981).
13. W. Hage, K. Wisshak, F. Kaeppeler, Nucl. Sci. Eng. **78**, 248 (1981).
14. J.W.T.Dabbs, C.H.Johnson, C.E.Bemis Jr, Nucl. Sci. Eng. **83** 22 (1983).
15. P.E. Vorotnikov, S.V. Dmitriev, Yu.D. Molchanov, G.A. Otroshchenko, Yad. Fiz. **44**, 1403 (1986).
16. C. Borcea *et al.*, Nucl. Instrum. Methods A **513**, 524 (2003).
17. The n_TOF Collaboration (U. Abbondanno *et al.*), CERN n_TOF facility: Performance report, Technical report CERNSL-2002-053 ECT, CERN, Switzerland (2003).
18. The n_TOF Collaboration (U. Abbondanno *et al.*), Nucl. Instrum. Methods A **538**, 692 (2005).
19. The n_TOF Collaboration (G. Lorusso *et al.*), Nucl. Instrum. Methods A **532**, 622 (2004).
20. A. Fassò, A. Ferrari, J. Ranft, P.R. Sala, Technical report CERN-2005-10, CERN, Switzerland (2005).
21. M. Calviani *et al.*, Nucl. Instrum. Methods A **594**, 220 (2008).
22. P. Hofmann *et al.*, Phys. Rev. C **49**, 2555 (1994) G.D. Adveev *et al.*, Preprint INR 816/93 (1993).
23. The n_TOF Collaboration (F. Belloni *et al.*), Eur. Phys. J. A **47**, 160 (2011).
24. F. Belloni, PhD thesis, Università di Trieste (2010).
25. A.D. Carlson, V.G. Pronyaev, D.L. Smith, N.M. Larson, Zhenpeng Chen, G.M. Hale, F.-J. Hambsch, E.V. Gai, Soo-Youl Oh, S.A. Badikov, T. Kawano, H.M. Hofmann, H. Vonach, S. Tagesen, Nucl. Data Sheets **110**, 3215 (2009).
26. M.B. Chadwick *et al.*, Nucl. Data Sheets **107**, 2931 (2006).
27. M.B. Chadwick *et al.*, Nucl. Data Sheets **112**, 2887 (2011).
28. For results compiled in evaluated nuclear data libraries see, for example, *International Atomic Energy Agency (IAEA)* on `www-nds.iaea.org`, and the *OECD Nuclear Energy Agency* on `www.nea.fr/html/dbdata/`.
29. M. Herman, R. Capote, B.V. Carlson, P. Obložinský, M. Sin, A. Trkov, H. Wienke, V. Zerkin, Nucl. Data Sheets **108**, 2655 (2007).
30. D. Rochman, M. Herman, P. Obložinský, M. Sin, Nucl. Sci. Eng. **154**, 280 (2006).